Neutrino Experiments with Liquid Scintillator Detectors

An Overview

Daniel Bick

Institut für Experimentalphysik
Hamburg University

Hamburg Student Seminar, October 29th 2007

1. Neutrinos
   - General facts
   - Neutrino Mixing
   - Neutrinos
2. Detection principles
   - Neutrino detection
   - Liquid Scintillators
   - What can be investigated
3. Experiments
   - KamLAND
   - Borexino
   - Propects
4. Summary

1. Neutrinos
   - General facts
   - Neutrino Mixing
   - Neutrinos
2. Detection principles
   - Neutrino detection
   - Liquid Scintillators
   - What can be investigated
3. Experiments
   - KamLAND
   - Borexino
   - Propects
4. Summary

Some general aspects on the neutrino

- The (electron-)neutrino was predicted by Wolfgang Pauli in 1930.
- It was experimentally discovered in 1956 by Reines and Cowan.
- There is one corresponding neutrino for each charged lepton.

$$\begin{pmatrix} \nu_e \\ e^- \end{pmatrix} \qquad \begin{pmatrix} \nu_\mu \\ \mu^- \end{pmatrix} \qquad \begin{pmatrix} \nu_\tau \\ \tau^- \end{pmatrix}$$

Neutrinos Sources

Many neutrino sources - both natural and man made - exist:

- β-decays (up to some MeV)
- Atmospheric neutrinos ν_μ, $\bar{\nu}_\mu$, ν_e, $\bar{\nu}_e$ from π-decays (100 MeV - 10 TeV)
- Solar neutrinos: ν_e (< 2 MeV)
- Reactor neutrinos: $\bar{\nu}_e$ (up to 10 MeV)
- Neutrino beams: mainly ν_μ (some 10 GeV)
- Geoneutrinos: $\bar{\nu}_e$ (< 3.3 MeV)
- Supernovae: all flavors (some 10 MeV)
  - Supernova bursts
  - Relic neutrinos

Neutrino Mixing

- Neutrino flavor eigenstates $|\nu_\alpha\rangle$ differ from their mass eigenstates $|\nu_i\rangle$.
- There are three mass eigenstates ν_1, ν_2, ν_3 corresponding to the charged-lepton mass eigenstates e, μ and τ.
- Eigenstates are connected by the mixing matrix U_{PMNS}.

$$|\nu_i\rangle = \sum_\alpha U_{i\alpha}|\nu_\alpha\rangle \qquad |\nu_\alpha\rangle = \sum_i U^*_{i\alpha}|\nu_i\rangle.$$

Neutrino propagation

The propagation of the mass eigenstates is described by:

$$|\nu_i(t)\rangle = e^{E_i t - \mathbf{p}_i \mathbf{L}} |\nu_i(0)\rangle = e^{-i\frac{m_i^2}{2E}L} |\nu_i(0)\rangle$$

$$P_{\nu_\alpha \to \nu_\beta} = \left| \sum_i \left\langle \nu_\alpha \left| e^{-i\frac{m_i^2}{2E}L} \right| \nu_\beta \right\rangle \right|^2$$

Neutrino mixing leads to oscillations.

$$P_{\nu_\alpha \to \nu_\beta} = \delta_{\alpha\beta} - 4 \sum_{i>j} \mathrm{Re}(U_{\alpha i}^* U_{\beta i} U_{\alpha j} U_{\beta j}^*) \sin^2 \left(\Delta m_{ij}^2 \frac{L}{4E} \right)$$
$$+ 2 \sum_{i>j} \mathrm{Im}(U_{\alpha i}^* U_{\beta i} U_{\alpha j} U_{\beta j}^*) \sin \left(\Delta m_{ij}^2 \frac{L}{2E} \right)$$

With $\Delta m_{ij}^2 = m_i^2 - m_j^2$

The mixing matrix

$$U = \overbrace{\begin{pmatrix} 1 & 0 & 0 \\ 0 & \cos\theta_{23} & \sin\theta_{23} \\ 0 & -\sin\theta_{23} & \cos\theta_{23} \end{pmatrix}}^{\text{atmospheric}} \times \overbrace{\begin{pmatrix} \cos\theta_{13} & 0 & \sin\theta_{13} e^{-i\delta} \\ 0 & 1 & 0 \\ -\sin\theta_{13} e^{i\delta} & 0 & \cos\theta_{13} \end{pmatrix}}^{\text{cross-mixing}}$$

$$\times \underbrace{\begin{pmatrix} \cos\theta_{12} & \sin\theta_{12} & 0 \\ -\sin\theta_{12} & \cos\theta_{12} & 0 \\ 0 & 0 & 1 \end{pmatrix}}_{\text{solar}} \times \underbrace{\begin{pmatrix} e^{i\alpha_1/2} & 0 & 0 \\ 0 & e^{i\alpha_2/2} & 0 \\ 0 & 0 & 1 \end{pmatrix}}_{\text{majorana phases}}$$

$$U = \begin{pmatrix} c_{12}c_{13} & s_{12}c_{13} & s_{13}e^{-i\delta} \\ -s_{12}c_{23} - c_{12}s_{23}s_{13}e^{i\delta} & c_{12}c_{23} - s_{12}s_{23}s_{13}e^{i\delta} & s_{23}c_{13} \\ s_{12}s_{23} - c_{12}c_{23}s_{13}e^{i\delta} & -c_{12}s_{23} - s_{12}c_{23}s_{13}e^{i\delta} & c_{23}c_{13} \end{pmatrix}$$

The mixing matrix

$$U = \overbrace{\begin{pmatrix} 1 & 0 & 0 \\ 0 & \cos\theta_{23} & \sin\theta_{23} \\ 0 & -\sin\theta_{23} & \cos\theta_{23} \end{pmatrix}}^{\text{atmospheric}} \times \overbrace{\begin{pmatrix} \cos\theta_{13} & 0 & \sin\theta_{13} e^{-i\delta} \\ 0 & 1 & 0 \\ -\sin\theta_{13} e^{i\delta} & 0 & \cos\theta_{13} \end{pmatrix}}^{\text{cross-mixing}}$$
$$\times \underbrace{\begin{pmatrix} \cos\theta_{12} & \sin\theta_{12} & 0 \\ -\sin\theta_{12} & \cos\theta_{12} & 0 \\ 0 & 0 & 1 \end{pmatrix}}_{\text{solar}}$$

$$U = \begin{pmatrix} c_{12}c_{13} & s_{12}c_{13} & s_{13}e^{-i\delta} \\ -s_{12}c_{23} - c_{12}s_{23}s_{13}e^{i\delta} & c_{12}c_{23} - s_{12}s_{23}s_{13}e^{i\delta} & s_{23}c_{13} \\ s_{12}s_{23} - c_{12}c_{23}s_{13}e^{i\delta} & -c_{12}s_{23} - s_{12}c_{23}s_{13}e^{i\delta} & c_{23}c_{13} \end{pmatrix}$$

The mixing matrix

$$U = \overbrace{\begin{pmatrix} 1 & 0 & 0 \\ 0 & \cos\theta_{23} & \sin\theta_{23} \\ 0 & -\sin\theta_{23} & \cos\theta_{23} \end{pmatrix}}^{\text{atmospheric}} \times \overbrace{\begin{pmatrix} \cos\theta_{13} & 0 & \sin\theta_{13} e^{-i\delta} \\ 0 & 1 & 0 \\ -\sin\theta_{13} e^{i\delta} & 0 & \cos\theta_{13} \end{pmatrix}}^{\text{cross-mixing}}$$
$$\times \underbrace{\begin{pmatrix} \cos\theta_{12} & \sin\theta_{12} & 0 \\ -\sin\theta_{12} & \cos\theta_{12} & 0 \\ 0 & 0 & 1 \end{pmatrix}}_{\text{solar}}$$

$$U = \begin{pmatrix} c_{12}c_{13} & s_{12}c_{13} & s_{13}e^{-i\delta} \\ -s_{12}c_{23} - c_{12}s_{23}s_{13}e^{i\delta} & c_{12}c_{23} - s_{12}s_{23}s_{13}e^{i\delta} & s_{23}c_{13} \\ s_{12}s_{23} - c_{12}c_{23}s_{13}e^{i\delta} & -c_{12}s_{23} - s_{12}c_{23}s_{13}e^{i\delta} & c_{23}c_{13} \end{pmatrix}$$

Matter Effects (simplified)

Oscilliation in matter differs from vacuum oscillatons:
Coherent forward scattering of neutrinos from particles along their way can have an effect.

- Coherent forward scattering via W exchange occurs for electron type neutrinos.
- Scattering via Z exchange for all neutrino types $\rightarrow$ effect cancels out.

This means that neutrinos in matter have a different effective mass than neutrinos in vacuum!

- Matter effects depend on the neutrino energy. Larger effect for more energetic neutrinos.

Detection methods

Three major methods of detecting neutrinos:

- Čerenkov Detectors
  ($E_{\mathrm{thr}} \simeq 5\,\mathrm{MeV}$).
- Radiochemical Detectors
  (e.g. C_2Cl_4: $E_{\mathrm{thr}} = 814\,\mathrm{keV}$, Ga: $E_{\mathrm{thr}} = 233\,\mathrm{keV}$).
  No energy measurement possible.
- Liquid Scintillation Detectors
  ($E_{\mathrm{thr}} \simeq 200\,\mathrm{keV}$ for ν and $E_{\mathrm{thr}} \simeq 1.8\,\mathrm{MeV}$ for $\bar{\nu}$)

Liquid Scintillators

- Organic liquid scintillators are aromatic hydrocarbon compunds containing benzene-ring structures.
- Passing particles deposit ionizing energy in the scintillator, exciting the free valence electrons of the benzene-rings.
- Scintillation light is emitted due to transitions from excited states to the ground state.

$\bar{\nu}_e$-detection via the inverse β-decay

Inverse β decay on protons:

$$p + \bar{\nu}_e \longrightarrow e^+ + n$$

- CC reaction of a proton and an antineutrino. (cross section in the order of $10^{-42}\,\mathrm{cm}^2$).
- The positron anihilates with some electron imediately emitting two γ's. Visible energy: $E_{\text{prompt}} = E_{\bar{\nu}_e} - \bar{E}_n - 0.8\,\text{MeV}$
- The neutron will be captured after a short delay (typically around $200\,\mu\text{s}$), releasing $2.2\,\text{MeV}$.
- Coincidence signal between the prompt positron and the gammas from the delayed neutron-capture.

Reaction threshold:

$$E_{\nu,\min} = \frac{(M_n + M_e)^2 - M_p^2}{2M_p} = 1.806\,\text{MeV}.$$

$\bar{\nu}_e$-detection via the inverse β-decay

Inverse β decay on protons:

$$p + \bar{\nu}_e \longrightarrow e^+ + n$$

- CC reaction of a proton and an antineutrino. (cross section in the order of $10^{-42}\,\mathrm{cm}^2$).
- The positron anihilates with some electron imediately emitting two γ's. Visible energy: $E_{\mathrm{prompt}} = E_{\bar{\nu}_e} - \bar{E}_n - 0.8\,\mathrm{MeV}$
- The neutron will be captured after a short delay (typically around $200\,\mu\mathrm{s}$), releasing $2.2\,\mathrm{MeV}$.
- Coincidence signal between the prompt positron and the gammas from the delayed neutron-capture.

Reaction threshold:

$$E_{\nu,\mathrm{min}} = \frac{(M_n + M_e)^2 - M_p^2}{2M_p} = 1.806\,\mathrm{MeV}.$$

$\bar{\nu}_e$-detection via the inverse β-decay

Inverse β decay on protons:

$$p + \bar{\nu}_e \longrightarrow e^+ + n$$

- CC reaction of a proton and an antineutrino. (cross section in the order of $10^{-42}\,\mathrm{cm}^2$).
- The positron anihilates with some electron imediately emitting two γ's. Visible energy: $E_{\mathrm{prompt}} = E_{\bar{\nu}_e} - \bar{E}_n - 0.8\,\mathrm{MeV}$
- The neutron will be captured after a short delay (typically around 200 μs), releasing 2.2 MeV.
- Coincidence signal between the prompt positron and the gammas from the delayed neutron-capture.

Reaction threshold:

$$E_{\nu,\mathrm{min}} = \frac{(M_n + M_e)^2 - M_p^2}{2M_p} = 1.806\,\mathrm{MeV}.$$

$\bar{\nu}_e$-detection via the inverse β-decay

Inverse β decay on protons:

$$p + \bar{\nu}_e \longrightarrow e^+ + n$$

- CC reaction of a proton and an antineutrino. (cross section in the order of $10^{-42}\,\text{cm}^2$).
- The positron anihilates with some electron imediately emitting two γ's. Visible energy: $E_{\text{prompt}} = E_{\bar{\nu}_e} - \bar{E}_n - 0.8\,\text{MeV}$
- The neutron will be captured after a short delay (typically around $200\,\mu$s), releasing 2.2 MeV.
- Coincidence signal between the prompt positron and the gammas from the delayed neutron-capture.

Reaction threshold:

$$E_{\nu,\text{min}} = \frac{(M_n + M_e)^2 - M_p^2}{2M_p} = 1.806\,\text{MeV}.$$

$\bar{\nu}_e$-detection via the inverse β-decay

Inverse β decay on protons:

$$p + \bar{\nu}_e \longrightarrow e^+ + n$$

- CC reaction of a proton and an antineutrino. (cross section in the order of $10^{-42}\,\text{cm}^2$).
- The positron anihilates with some electron imediately emitting two γ's. Visible energy: $E_{\text{prompt}} = E_{\bar{\nu}_e} - \bar{E}_n - 0.8\,\text{MeV}$
- The neutron will be captured after a short delay (typically around $200\,\mu$s), releasing $2.2\,$MeV.
- Coincidence signal between the prompt positron and the gammas from the delayed neutron-capture.

Reaction threshold:

$$E_{\nu,\text{min}} = \frac{(M_n + M_e)^2 - M_p^2}{2M_p} = 1.806\,\text{MeV}.$$

$\bar{\nu}_e$-detection via the inverse β-decay

Inverse β decay on protons:

$$p + \bar{\nu}_e \longrightarrow e^+ + n$$

- CC reaction of a proton and an antineutrino. (cross section in the order of $10^{-42}\,\mathrm{cm}^2$).
- The positron anihilates with some electron imediately emitting two γ's. Visible energy: $E_{\text{prompt}} = E_{\bar{\nu}_e} - \bar{E}_n - 0.8\,\mathrm{MeV}$
- The neutron will be captured after a short delay (typically around $200\,\mu$s), releasing $2.2\,\mathrm{MeV}$.
- Coincidence signal between the prompt positron and the gammas from the delayed neutron-capture.

Reaction threshold:

$$E_{\nu,\min} = \frac{(M_n + M_e)^2 - M_p^2}{2M_p} = 1.806\,\mathrm{MeV}.$$

ν-detection via elastic scattering

The process

$$\nu_x + e^- \rightarrow \nu_x + e^-$$

is sensitive to all neutrino flavors.

- Cross section 6 times higher for electron type neutrinos.
- Scattered electrons are detected by means of the scintillation light produced in the liquid scintillator.
- Recoil electron profile is similar to that of Compton scattering of γ-rays.
- Sensitive to low energies

ν-detection via elastic scattering

The process

$$\nu_x + e^- \longrightarrow \nu_x + e^-$$

is sensitive to all neutrino flavors.

- Cross section 6 times higher for electron type neutrinos.
- Scattered electrons are detected by means of the scintillation light produced in the liquid scintillator.
- Recoil electron profile is similar to that of Compton scattering of γ-rays.
- Sensitive to low energies

ν-detection via elastic scattering

The process

$$\nu_x + e^- \longrightarrow \nu_x + e^-$$

is sensitive to all neutrino flavors.

- Cross section 6 times higher for electron type neutrinos.
- Scattered electrons are detected by means of the scintillation light produced in the liquid scintillator.
- Recoil electron profile is similar to that of Compton scattering of γ-rays.
- Sensitive to low energies

ν-detection via elastic scattering

The process

$$\nu_x + e^- \longrightarrow \nu_x + e^-$$

is sensitive to all neutrino flavors.

- Cross section 6 times higher for electron type neutrinos.
- Scattered electrons are detected by means of the scintillation light produced in the liquid scintillator.
- Recoil electron profile is similar to that of Compton scattering of γ-rays.
- Sensitive to low energies

ν-detection via elastic scattering

The process

$$\nu_x + e^- \longrightarrow \nu_x + e^-$$

is sensitive to all neutrino flavors.

- Cross section 6 times higher for electron type neutrinos.
- Scattered electrons are detected by means of the scintillation light produced in the liquid scintillator.
- Recoil electron profile is similar to that of Compton scattering of γ-rays.
- Sensitive to low energies

The perfect mixture?

A typical scintillator us usually made of:

- A solvent serving as a target and as a source of scintillation light.
- One or more fluors (a few g per l).

The solvent is in general not transparent for its own scintillation light. Therefore wavelength shifters (also denoted as fluors) are added.

For the delayed neutron capture when detecting antineutrinos, it's of advantage to add a target element such as Gd to the LS.

Properties of LS

- The light yield describes the number of photons emitted by the scintillator per amount of deposited energy by an incoming ionizing particle.
- Sometimes also expresses in the corresponding number of pe. In modern LS, about 400 photoelectrons per MeV are feasible.
- The attenuation length combines scattering and absorbtion effects reducing the average distance scintillation light is able to propagate.
- Typical values vary around 10 m

Properties of LS

- The light yield describes the number of photons emitted by the scintillator per amount of deposited energy by an incoming ionizing particle.
- Sometimes also expresses in the corresponding number of pe. In modern LS, about 400 photoelectrons per MeV are feasible.
- The attenuation length combines scattering and absorbtion effects reducing the average distance scintillation light is able to propagate.
- Typical values vary around 10 m

Energy reconstruction

The energy can be obtained from the number of observed photoelectrons (p.e.) in PMTs.
Corrections to take into account:

- density of PMTs
- shadows from the geometry (eg. suspension ropes)
- transparencies of LS and other liquids involved.

Project Poltergeist

First experimental evidence of neutrinos was given in the Project Poltergeist experiment in 1956.

- A solvent of Water and $CdCl_2$ was used as a target.
- Two liquid scintillation counters were placed next to it

Organic LS have been THE detection medium of choice for antineutrinos since the early discovery experiment of Reines and Cowan.

Observations done with LS

Liquid scintillators already offer a large and intresting spectrum of possible obervations:

- Solar neutrinos (test SSM, look for oscillations)
- Reactor neutrinos ($E_{\bar{\nu}_e} > 1.8\,\mathrm{MeV}$)
- Neutrinos from inside the Earth (Geoneutrinos)

Neutrinos from the Sun: pp-chain

Energy production in the Sun through fusion:

$$p + p \rightarrow d + e^+ + \nu_e \quad (pp) \qquad p + e^- + p \rightarrow d + \nu_e \quad (pep)$$

$$d + p \rightarrow {}^3\mathrm{He} + \gamma$$

pp I:

$${}^3\mathrm{He} + {}^3\mathrm{He} \rightarrow {}^4\mathrm{He} + p + p$$

pp II:

$$\begin{aligned} {}^3\mathrm{He} + {}^4\mathrm{He} &\rightarrow {}^7\mathrm{Be} + \gamma \\ {}^7\mathrm{Be} + e^- &\rightarrow {}^7\mathrm{Li} + \nu_e \\ {}^7\mathrm{Li} + p &\rightarrow {}^4\mathrm{He} + {}^4\mathrm{He} \end{aligned}$$

pp III:

$$\begin{aligned} {}^3\mathrm{He} + {}^4\mathrm{He} &\rightarrow {}^7\mathrm{Be} + \gamma \\ {}^7\mathrm{Be} + {}^1\mathrm{H} &\rightarrow {}^8\mathrm{B} + \gamma \\ {}^8\mathrm{B} &\rightarrow {}^8\mathrm{Be} + e^+ + \nu_e \\ {}^8\mathrm{Be} &\leftrightarrow {}^4\mathrm{He} + {}^4\mathrm{He} \end{aligned}$$

pp IV / HEP:

$${}^3\mathrm{He} + {}^1\mathrm{H} \rightarrow {}^4\mathrm{He} + \nu_e + e^+$$

Neutrinos from the Sun: pp-chain

Energy production in the Sun through fusion:

$$p + p \rightarrow d + e^+ + \nu_e \quad (pp) \qquad p + e^- + p \rightarrow d + \nu_e \quad (pep)$$

$$d + p \rightarrow {}^3\mathrm{He} + \gamma$$

pp I:

$${}^3\mathrm{He} + {}^3\mathrm{He} \rightarrow {}^4\mathrm{He} + p + p$$

pp II:

$${}^3\mathrm{He} + {}^4\mathrm{He} \rightarrow {}^7\mathrm{Be} + \gamma$$

$${}^7\mathrm{Be} + e^- \rightarrow {}^7\mathrm{Li} + \nu_e$$

$${}^7\mathrm{Li} + p \rightarrow {}^4\mathrm{He} + {}^4\mathrm{He}$$

pp III:

$${}^3\mathrm{He} + {}^4\mathrm{He} \rightarrow {}^7\mathrm{Be} + \gamma$$

$${}^7\mathrm{Be} + {}^1\mathrm{H} \rightarrow {}^8\mathrm{B} + \gamma$$

$${}^8\mathrm{B} \rightarrow {}^8\mathrm{Be} + e^+ + \nu_e$$

$${}^8\mathrm{Be} \leftrightarrow {}^4\mathrm{He} + {}^4\mathrm{He}$$

pp IV / HEP:

$${}^3\mathrm{He} + {}^1\mathrm{H} \rightarrow {}^4\mathrm{He} + \nu_e + e^+$$

Neutrinos from the Sun: pp-chain

Energy production in the Sun through fusion:

$$p + p \longrightarrow d + e^{+} + \nu_e \quad (pp) \qquad p + e^{-} + p \longrightarrow d + \nu_e \quad (pep)$$

$$d + p \longrightarrow {}^{3}\mathrm{He} + \gamma$$

pp I:

$${}^{3}\mathrm{He} + {}^{3}\mathrm{He} \longrightarrow {}^{4}\mathrm{He} + p + p$$

pp II:

$${}^{3}\mathrm{He} + {}^{4}\mathrm{He} \longrightarrow {}^{7}\mathrm{Be} + \gamma$$

$${}^{7}\mathrm{Be} + e^{-} \longrightarrow {}^{7}\mathrm{Li} + \nu_e$$

$${}^{7}\mathrm{Li} + p \longrightarrow {}^{4}\mathrm{He} + {}^{4}\mathrm{He}$$

pp III:

$${}^{3}\mathrm{He} + {}^{4}\mathrm{He} \longrightarrow {}^{7}\mathrm{Be} + \gamma$$

$${}^{7}\mathrm{Be} + {}^{1}\mathrm{H} \longrightarrow {}^{8}\mathrm{B} + \gamma$$

$${}^{8}\mathrm{B} \longrightarrow {}^{8}\mathrm{Be} + e^{+} + \nu_e$$

$${}^{8}\mathrm{Be} \longleftrightarrow {}^{4}\mathrm{He} + {}^{4}\mathrm{He}$$

pp IV / HEP:

$${}^{3}\mathrm{He} + {}^{1}\mathrm{H} \longrightarrow {}^{4}\mathrm{He} + \nu_e + e^{+}$$

CNO cycle / neutrino spectrum

CNO:

$$^{12}C + {}^{1}H \rightarrow {}^{13}N + \gamma$$
$$^{13}N \rightarrow {}^{13}C + e^{+} + \nu_e$$
$$^{13}C + {}^{1}H \rightarrow {}^{14}N + \gamma$$
$$^{14}N + {}^{1}H \rightarrow {}^{15}O + \gamma$$
$$^{15}O \rightarrow {}^{15}N + e^{+} + \nu_e$$
$$^{15}N + {}^{1}H \rightarrow {}^{12}C + {}^{4}He$$

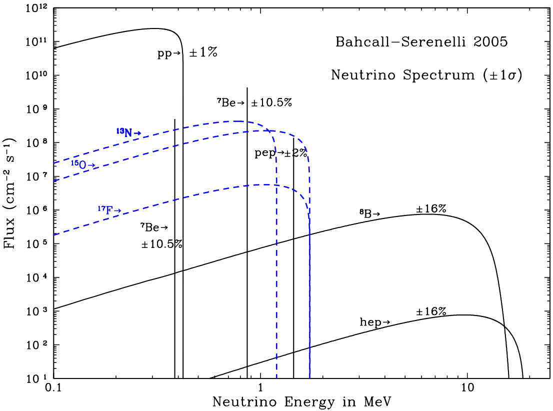

CNO cycle / neutrino spectrum

CNO:

$$^{12}\mathrm{C} + {}^{1}\mathrm{H} \rightarrow {}^{13}\mathrm{N} + \gamma$$
$$^{13}\mathrm{N} \rightarrow {}^{13}\mathrm{C} + e^{+} + \nu_e$$
$$^{13}\mathrm{C} + {}^{1}\mathrm{H} \rightarrow {}^{14}\mathrm{N} + \gamma$$
$$^{14}\mathrm{N} + {}^{1}\mathrm{H} \rightarrow {}^{15}\mathrm{O} + \gamma$$
$$^{15}\mathrm{O} \rightarrow {}^{15}\mathrm{N} + e^{+} + \nu_e$$
$$^{15}\mathrm{N} + {}^{1}\mathrm{H} \rightarrow {}^{12}\mathrm{C} + {}^{4}\mathrm{He}$$

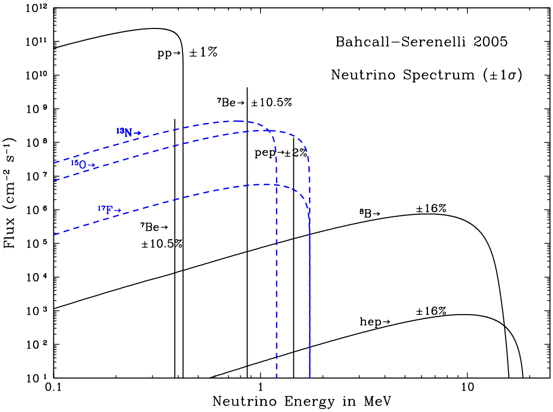

CNO cycle / neutrino spectrum

CNO:

$$^{12}\text{C} + {}^{1}\text{H} \rightarrow {}^{13}\text{N} + \gamma$$
$$^{13}\text{N} \rightarrow {}^{13}\text{C} + e^{+} + \nu_e$$
$$^{13}\text{C} + {}^{1}\text{H} \rightarrow {}^{14}\text{N} + \gamma$$
$$^{14}\text{N} + {}^{1}\text{H} \rightarrow {}^{15}\text{O} + \gamma$$
$$^{15}\text{O} \rightarrow {}^{15}\text{N} + e^{+} + \nu_e$$
$$^{15}\text{N} + {}^{1}\text{H} \rightarrow {}^{12}\text{C} + {}^{4}\text{He}$$

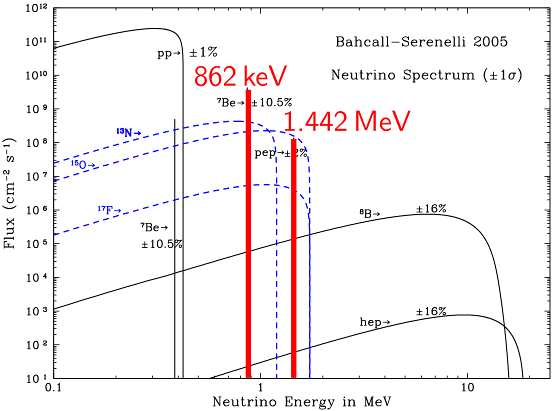

Observation of solar neutrinos

Fluxes and energies are predicted by the SSM:

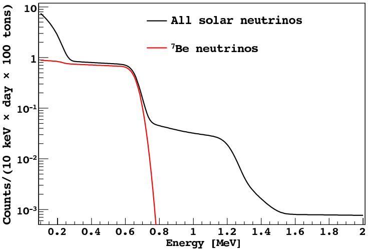

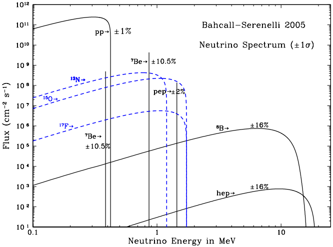

Neutrinos can be detected in a LS through elastic scattering:

$$\nu_x + e^- \rightarrow \nu_x + e^-$$

Clear Compton edge from recoil electron is expected.

Reactor neutrinos

- $\bar{\nu}_e$ are produced in nuclear reactors by beta decays of daughter nuclei from 4 fissile nuclei: mainly ^{235}U,^{239}Pu and also ^{238}U and ^{241}Pu.
- Neutrino sprectra from these components are well modeled by β-spectrum measurements for ^{235}U,^{239}Pu,^{238}U and theoretical calculations for ^{241}Pu.
- Approx. 6 $\bar{\nu}_e$ result from each fission event leading to 2×10^{20} $\bar{\nu}_e$ per GW$_{\text{th}}$ per second.
- Average energy of 3.7 MeV.
- $\bar{\nu}_e$ spectra known with an uncertainty of 2%.

$\Rightarrow$ Nuclear reactors are an excellent source for neutrinos.

Reactor neutrinos

- $\bar{\nu}_e$ are produced in nuclear reactors by beta decays of daughter nuclei from 4 fissile nuclei: mainly ^{235}U,^{239}Pu and also ^{238}U and ^{241}Pu.
- Neutrino sprectra from these components are well modeled by β-spectrum measurements for ^{235}U,^{239}Pu,^{238}U and theoretical calculations for ^{241}Pu.
- Approx. 6 $\bar{\nu}_e$ result from each fission event leading to 2×10^{20} $\bar{\nu}_e$ per GW$_{th}$ per second.
- Average energy of 3.7 MeV.
- $\bar{\nu}_e$ spectra known with an uncertainty of 2%.

$\Rightarrow$ Nuclear reactors are an excellent source for neutrinos.

Reactor neutrino flux

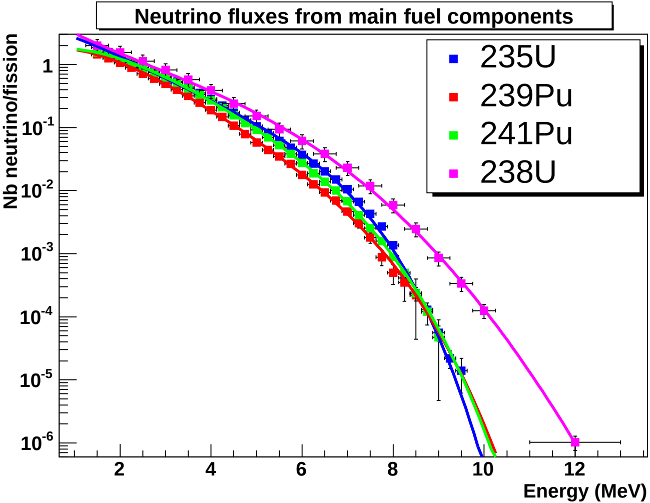

Geoneutrinos

- Heat flow from Earth measured to be approx 44 TW.
- Almost half the power from radioactivity of material inside Earth (16 TW)
- Geological studies: 84% produced by ^{238}U and ^{232}Th decays.

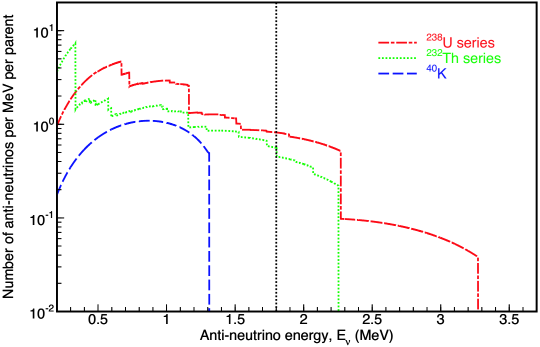

Geoneutrino detection

Detectable via inverse beta decay.
No direct angular information form liquid scintillator.

- Indirect directional determination because the final neutron is displaced in the forward direction.
- Offset between e^+ and neutron capture location can be determined
- Can be done by analyzing the arrival times and the number of photons for each PMT.

Hard to distinguish from reactor antineutrinos.

Geoneutrino detection - what can be found out?

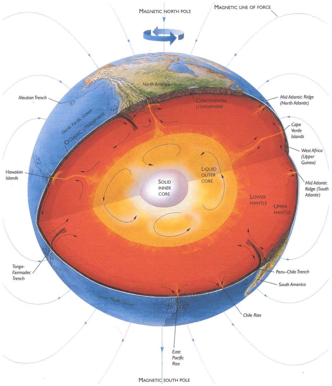

Get geophysical information:

- Get the distribution of radioactive elements in Earth
- Radioactive elements in core?
- Nuclear reactor in core?
- Interpretation of geomagnetism.

It would be too simple... without Background

Background mainly a problem for ν_x detection.

Cosmic:

- ^{11}C cosmogenic events from the reaction
  $\mu +^{12} \mathrm{C} + \text{secondaries} \rightarrow \mu +^{11} \mathrm{C} + n + \text{secondaries}$

Radioactive:

- ^{14}C: β^- end point energy: 156 keV
- ^{210}Po (daughter of ^{222}Rn), $T_{1/2} \approx 138\,\mathrm{d}$, deposits $\approx 350\,\mathrm{keV}$
- ^{85}Kr: β^- end point energy: 687.4 keV

KamLAND

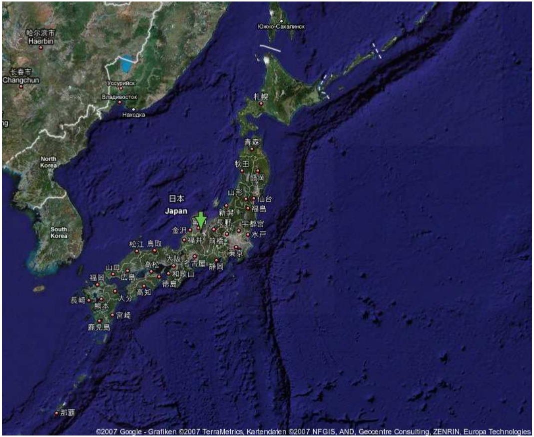

KamLAND -
Kamioka
Liquid Scintillator
Anti-**N**eutrino
Detector.

Kam LAND
Kamioka Liquid scintillator Anti-Neutrino Detector

KamLAND

- 53 commercial nuclear reactors in Japan
- Located at the former Kamiokande site.
- 70 GW of power is generated by nuclear reactors at distances between 130 and 220 km (7% of world total).
- This contributes to 80% of the total neutrino flux at the site.
- Inside Mt. Ikenoyama → 2700 m.w.e. rock shielding.

KamLAND

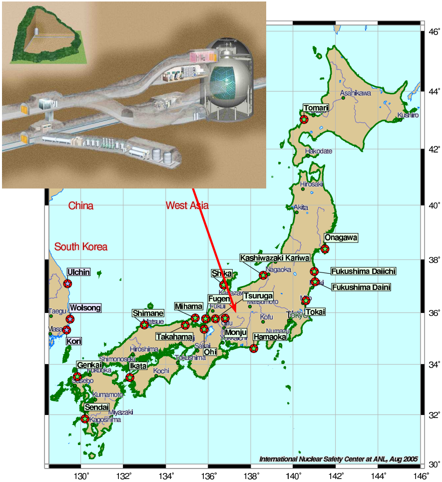

- 53 commercial nuclear reactors in Japan
- Located at the former Kamiokande site.
- 70 GW of power is generated by nuclear reactors at distances between 130 and 220 km (7% of world total).
- This contributes to 80% of the total neutrino flux at the site.
- Inside Mt. Ikenoyama → 2700 m.w.e. rock shielding.

KamLAND

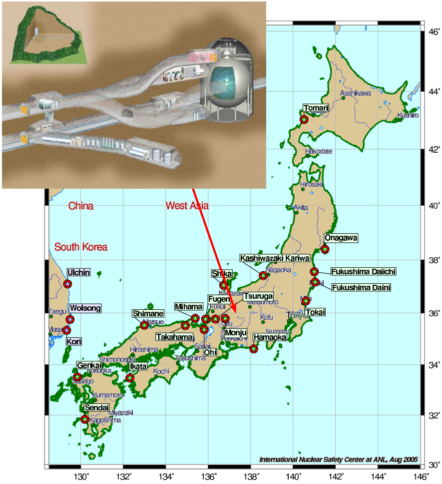

- 53 commercial nuclear reactors in Japan
- Located at the former Kamiokande site.
- 70 GW of power is generated by nuclear reactors at distances between 130 and 220 km (7% of world total).
- This contributes to 80% of the total neutrino flux at the site.
- Inside Mt. Ikenoyama → 2700 m.w.e. rock shielding.

KamLAND

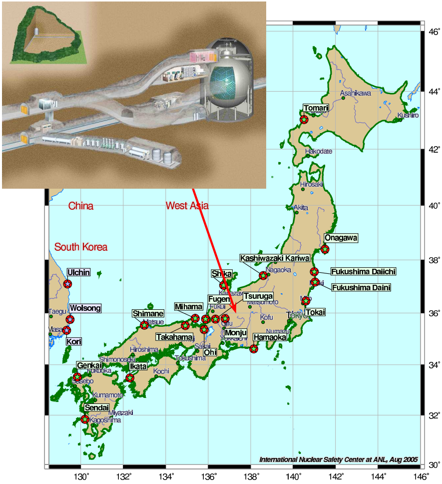

- 53 commercial nuclear reactors in Japan
- Located at the former Kamiokande site.
- 70 GW of power is generated by nuclear reactors at distances between 130 and 220 km (7% of world total).
- This contributes to 80% of the total neutrino flux at the site.
- Inside Mt. Ikenoyama → 2700 m.w.e. rock shielding.

KamLAND

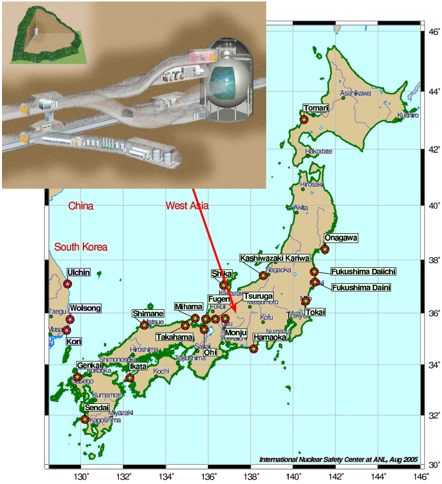

- 53 commercial nuclear reactors in Japan
- Located at the former Kamiokande site.
- 70 GW of power is generated by nuclear reactors at distances between 130 and 220 km (7% of world total).
- This contributes to 80% of the total neutrino flux at the site.
- Inside Mt. Ikenoyama $\rightarrow$ 2700 m.w.e. rock shielding.

Physics perspective

- Neutrino flux is approx. $6 \times 10^6/\mathrm{cm}^2/\mathrm{sec}$ at site.
- Opportunity to investigate $\bar{\nu}_e$ oscillations.

$$P_{\bar{\nu}_e \to \bar{\nu}_e} \approx 1 - \sin^2 2\theta_{12} \sin^2 \frac{\Delta m_{12}^2 L}{4E}$$

- 1 ton of ultrapure LS used to meausre $\bar{\nu}_e$ disappearance.

Physics perspective

- Neutrino flux is approx. $6 \times 10^6/\text{cm}^2/\text{sec}$ at site.
- Opportunity to investigate $\bar{\nu}_e$ oscillations.

$$P_{\bar{\nu}_e \to \bar{\nu}_e} \approx 1 - \sin^2 2\theta_{12} \sin^2 \frac{\Delta m_{12}^2 L}{4E}$$

- 1 ton of ultrapure LS used to meausre $\bar{\nu}_e$ disappearance.

Detector Design

$1200\,m^3$ liquid scintillator

- 20% 1,2,4-trimethylbenzene
- 80% dodecane ($C_{12}H_{26}$)
- Fluor: 1.52 g/l PPO (2,5-diphenyloxazole)

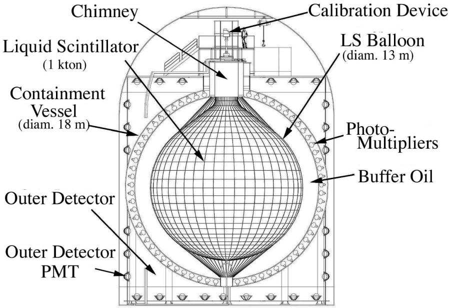

Detector Design

$1200\,m^3$ liquid scintillator

- target

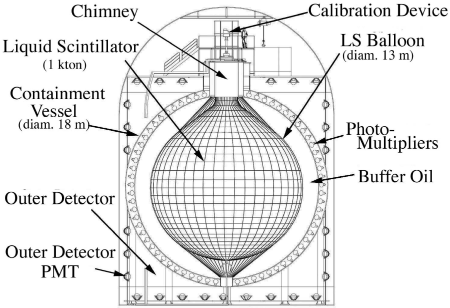

Detector Design

$1200\,m^3$ liquid scintillator

- target

$1800\,m^3$ buffer oil

- 50% dodecane
- 50% isoparaffin

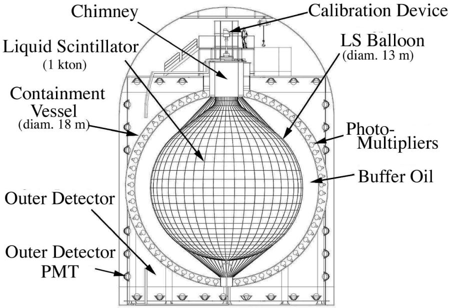

Detector Design

$1200\,m^3$ liquid scintillator

- target

$1800\,m^3$ buffer oil

- Schields target from external radiation, e.g. emitted by PMTs

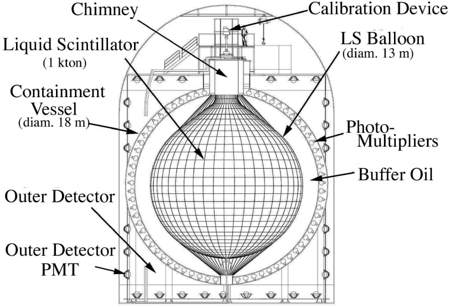

Detector Design

1200 m^3 liquid scintillator

- target

1800 m^3 buffer oil

- Schields target from external radiation, e.g. emitted by PMTs

Phototubes

- 1325 newly developed 17" tubes
- 554 old Kamiokande 20" tubes

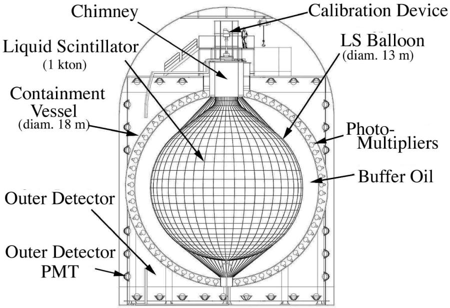

Detector Design

- $1200\,m^3$ liquid scintillator
  - target
- $1800\,m^3$ buffer oil
  - Schields target from external radiation, e.g. emitted by PMTs
- Phototubes
  - Photocoverage of 34%

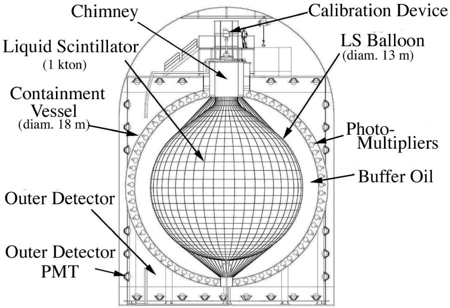

Detector Design

1200 m^3 liquid scintillator

- target

1800 m^3 buffer oil

- Schields target from external radiation, e.g. emitted by PMTs

Phototubes

- Photocoverage of 34%

Water Čerenkov detector

- 3.2 kton pure water
- 225 old Kamiokande 20" tubes

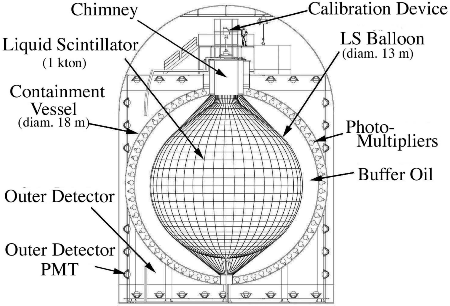

Detector Design

$1200\,\text{m}^3$ liquid scintillator

- target

$1800\,\text{m}^3$ buffer oil

- Schields target from external radiation, e.g. emitted by PMTs

Phototubes

- Photocoverage of 34%

Water Čerenkov detector

- Absorbs γ-rays and neutrons from surrounding rock and acts as a tag for cosmic muons.

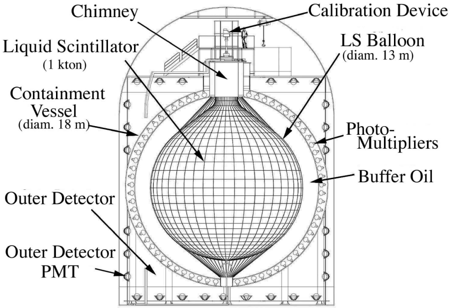

Performance

- e^+ and the delayed 2.2 MeV gamma from neutron capture on proton make a clear coincidence signal (mean neutron capture time 210 μs)
- Energy response calibrated with ^{68}Ge, ^{65}Zn, ^{60}Co and Am-Be γ-ray sources
- Event locations can be reconstructed from the timing of PMT hits with a typical resolution of $\approx$ 25 cm

Analysis

Trigger: 200 PMT hits corresponding to about 0.7 MeV.
Cuts:

- fiducial volume: $R < 5.5\,\mathrm{m}$
- time correlation ($0.5\mu\mathrm{s} < \Delta t < 660\,\mu\mathrm{s}$)
- delayed energy ($1.8\,\mathrm{MeV} < E_{\mathrm{delay}} < 2.6\,\mathrm{MeV}$)

$\Rightarrow$ Fiducial Volume contains 4.61×10^{31} free protons
$\Rightarrow$ Spatial resolution of 25 cm (Reconstructed from the timing of PMT hits)
Events with less than 10000 p.e. (approx. 30 MeV) and no prompt tag from the outer detector are candidates for reactor $\bar{\nu}_e$, more energetic events are muon candidates.

Oscillation Results

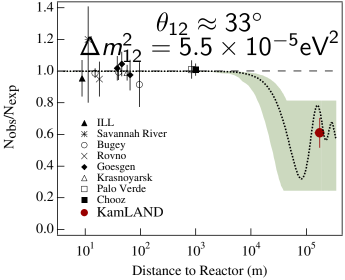

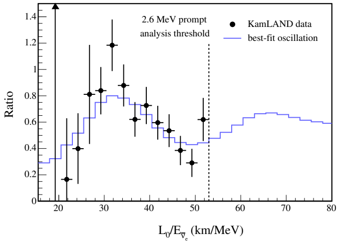

In 515.1 days of data taking smoking gun evidence for neutrino oscillation in the solar sector was found. 258 events were observed whereas 365.3 ± 23.7 would have been expected:

$$\Delta m^2_{12} = 7.9^{+0.6}_{-0.5} \times 10^{-5}\mathrm{eV}^2$$

More Oscillation Results

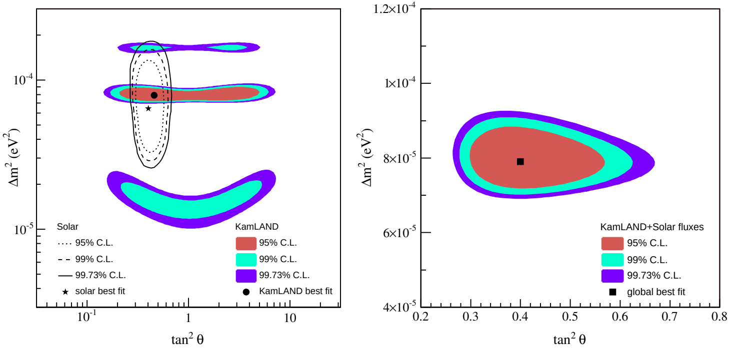

Combined with solar neutrino results the mixing angle θ_{12} can also be obtained

$$\tan^2\theta_{12} = 0.40^{+0.10}_{-0.07}$$

Geoneutrino observation

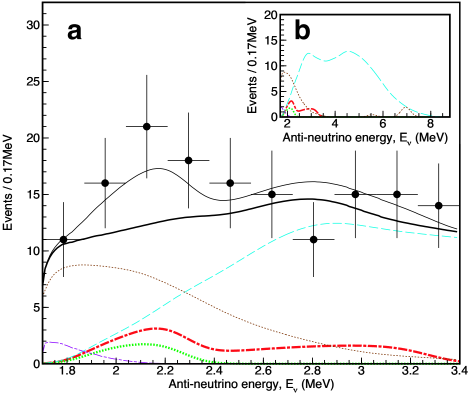

749 days of data taking:

$\bar{\nu}_e$ candidates:

- Observed: 152
- Estimated bg: 127 ± 13

bg sources:

- Reactor $\bar{\nu}_e$
- $^{13}C(\alpha, n)^{16}O$ (α from ^{210}Po)
- Random coincidences

Consistent with geophysical models.

Future prospects

- Purification of scintillator ongoing to get rid of ^{222}Rn contmination and the corresponding daughters eg. ^{210}Pb.
- ^{7}Be solar neutrino detection feasible.
- Not deep enough for *pep* detection (^{11}C bg)

Borexino

- Located at the Gran Sasso Laboratory in Italy
- Main goal: Detection of ^{7}Be solar neutrinos.

Borexino

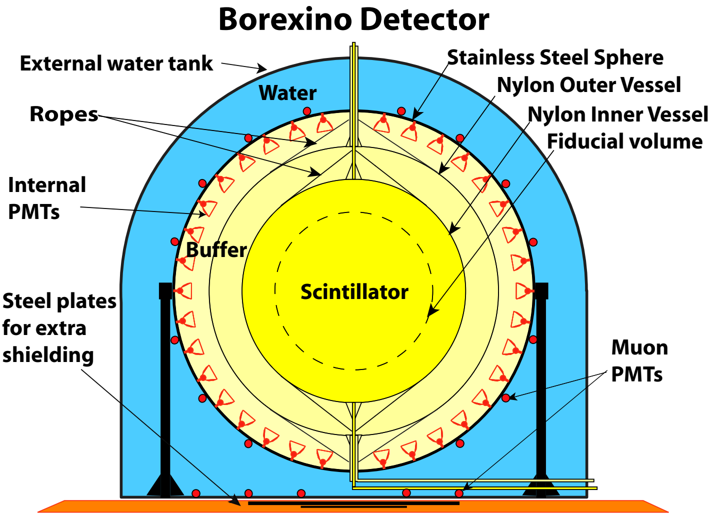
Borexino Detector
External water tank
Water
Stainless Steel Sphere
Nylon Outer Vessel
Nylon Inner Vessel
Fiducial volume
Ropes
Internal
PMTs
Buffer
Scintillator
Steel plates
for extra
shielding
Muon
PMTs

Detector Design

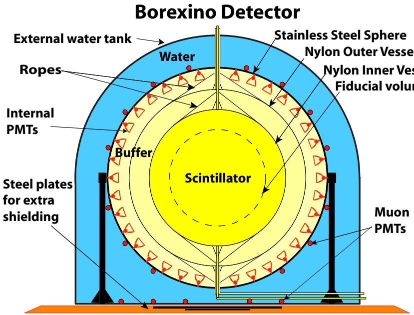

Inner Vessel:

- 300-ton liquid scintillator
- contained in an 125 μm nylon inner vessel
- Radius: 4.25 m
- LS: pseudocumene (PC, 1,2,4-trimethylbenzene)
- doped with PPO (2,5-diphenyloxazole) 1.5 g/l

Detector Design

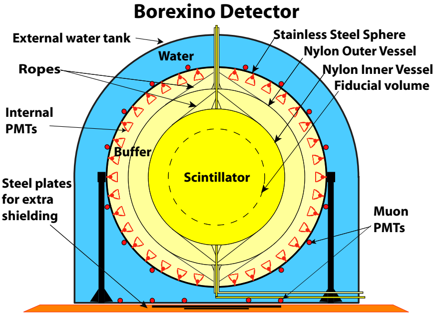

Outer Vessel:

- 5.5 m radius
- pseudocumene
- 5.0g/l DMP (dimethylphthalate) to quench scintillation.
- OV is barrier against radon and other background contaminations from outside.

Detector Design

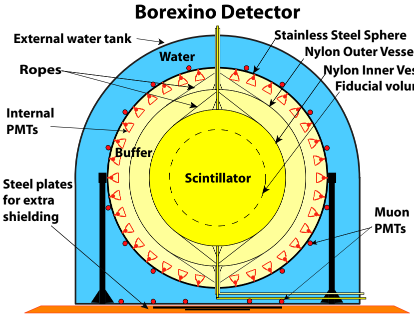

Stainless Steel Sphere

- Radius: 6.85 m
- Encloses PC-DMP buffer fluid.
- Support structure for PMTs

Detector Design

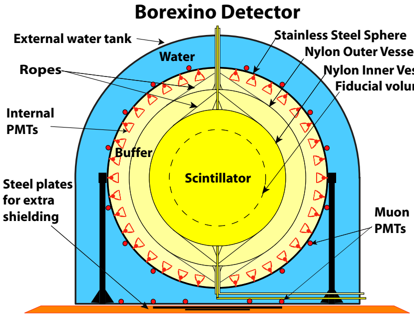

Outer Tank

- Radius of 9 m
- Height of 16.9 m
- Filled with ultra pure water
- 208 PMTs acting as a Čenrenkov muon detector

Detector Design

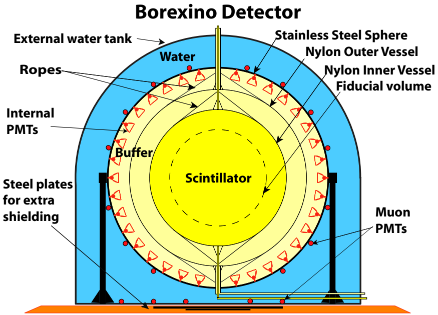

PMTs

- 2212 8" PMTs (ETL 9351)
- uniformly distributed on the inner surface of the SSS
- Mostly equipped with aluminum light concentrators

A view inside

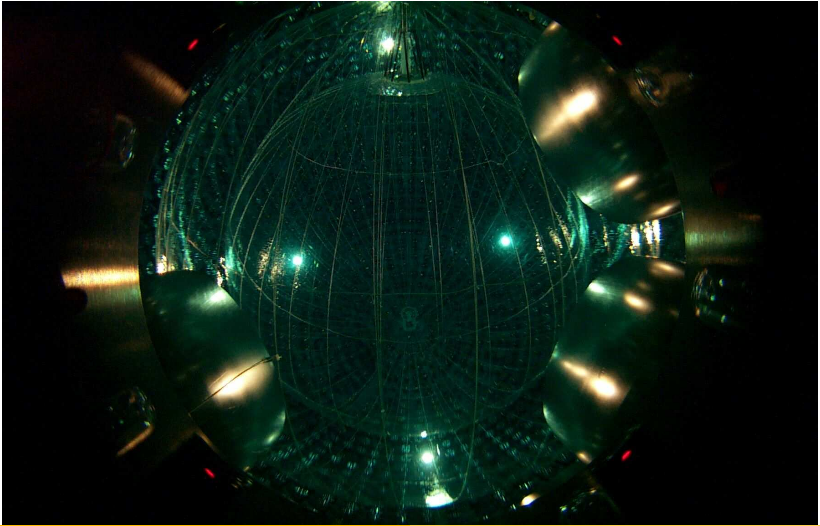

Detector properties

- Covered by 1400 m of rock or 3800 m.w.e.
- No nuclear reactors nearby.
- Approx. 5.5 m.w.e. shielding of the central volume from the rock.
- $\rightarrow$ Predicted γ background in the fiducial volume is less than 0.5 counts/(day $\cdot$ 100 tons).
- Optical attenuation length in the scintillator is approx. 7 m.
- Approx. 500 p.e./MeV are seen.
- Electrons from β^--decay of ^{14}C dominate the rate below 160 keV.
- Limits neutrino observation to energies above 200 keV.

Detector properties

- Covered by 1400 m of rock or 3800 m.w.e.
- No nuclear reactors nearby.
- Approx. 5.5 m.w.e. shielding of the central volume from the rock.
- $\rightarrow$ Predicted γ background in the fiducial volume is less than 0.5 counts/(day $\cdot$ 100 tons).
- Optical attenuation length in the scintillator is approx. 7 m.
- Approx. 500 p.e./MeV are seen.
- Electrons from β^--decay of ^{14}C dominate the rate below 160 keV.
- Limits neutrino observation to energies above 200 keV.

Detector properties

- Covered by 1400 m of rock or 3800 m.w.e.
- No nuclear reactors nearby.
- Approx. 5.5 m.w.e. shielding of the central volume from the rock.
- $\rightarrow$ Predicted γ background in the fiducial volume is less than 0.5 counts/(day · 100 tons).
- Optical attenuation length in the scintillator is approx. 7 m.
- Approx. 500 p.e./MeV are seen.
- Electrons from β^--decay of ^{14}C dominate the rate below 160 keV.
- Limits neutrino observation to energies above 200 keV.

Detection method

For detector monitoring and calibration all PMTs are illuminated every two seconds by a 394 nm laser pulse

Similar system using LEDs used for outer detector.

Monochromatic 862 keV neutrinos from ^{7}Be offer two signatures:

1. Recoil electron with a clear Compton edge at 665 keV.
2. $\pm$3.5% annual variation of the flux due to the Earth orbit eccentricity

Radio-purity

Only a very small contribution of external background.
The key requirement in the technology of Borexino is extremely low radioactive contamination.
Intrinsic bg-sources:

- ^{210}Po intrinsic to the scintillator. Peak at 350 keV.
- ^{85}Kr one of major uncertainties. Spectrum is similar to that of ^{7}Be recoil electron. The rate can be estimated from the decay to ^{85}Rb which is followed by a γ of 514 keV.
- ^{11}C is produced in reactions induced by cosmic muons. Signal between 1 and 2 MeV.
- ^{14}C content ratio ^{14}C/^{12}C of the order 10^{-18}. Dominate spectrum below 200 keV.

Radio-purity

Only a very small contribution of external background.
The key requirement in the technology of Borexino is extremely low radioactive contamination.
Intrinsic bg-sources:

- ^{210}Po intrinsic to the scintillator. Peak at 350 keV.
- ^{85}Kr one of major uncertainties. Spectrum is similar to that of ^{7}Be recoil electron. The rate can be estimated from the decay to ^{85}Rb which is followed by a γ of 514 keV.
- ^{11}C is produced in reactions induced by cosmic muons. Signal between 1 and 2 MeV.
- ^{14}C content ratio ^{14}C/^{12}C of the order 10^{-18}. Dominate spectrum below 200 keV.

Radio-purity

Only a very small contribution of external background.
The key requirement in the technology of Borexino is extremely low radioactive contamination.
Intrinsic bg-sources:

- ^{210}Po intrinsic to the scintillator. Peak at 350 keV.
- ^{85}Kr one of major uncertainties. Spectrum is similar to that of ^{7}Be recoil electron. The rate can be estimated from the decay to ^{85}Rb which is followed by a γ of 514 keV.
- ^{11}C is produced in reactions induced by cosmic muons. Signal between 1 and 2 MeV.
- ^{14}C content ratio ^{14}C/^{12}C of the order 10^{-18}. Dominate spectrum below 200 keV.

Radio-purity

Only a very small contribution of external background.
The key requirement in the technology of Borexino is extremely low radioactive contamination.
Intrinsic bg-sources:

- ^{210}Po intrinsic to the scintillator. Peak at 350 keV.
- ^{85}Kr one of major uncertainties. Spectrum is similar to that of ^{7}Be recoil electron. The rate can be estimated from the decay to ^{85}Rb which is followed by a γ of 514 keV.
- ^{11}C is produced in reactions induced by cosmic muons. Signal between 1 and 2 MeV.
- ^{14}C content ratio $^{14}C/^{12}C$ of the order 10^{-18}. Dominate spectrum below 200 keV.

Event Selection

Trigger conditions:

- Reject events with Čerenkov light
- Fiducial volume of 100 tons of LS
- $z < 1.8\,\mathrm{m}$ (removes bg from ^{222}Rn daughters in the upper inner vessel)
- 30 PMTs each detect at least one p.e. within a time of 60 ns
  For each pe the arrival time and the charge are measured during a time gate of $7.2\,\mu$s
  Typical trigger rate 15 Hz. (dominated by ^{14}C)

Results

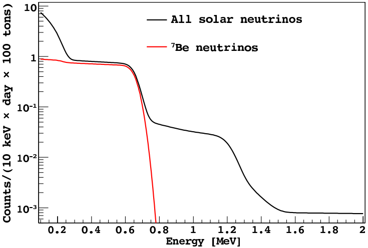

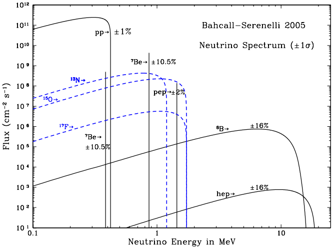

- ^{14}C dominates the spectrum for low energies.
- ^{210}Po peak at 200 pe is intrinsic to scintillator.
- Clear shoulder at 380 pe (approx 750 keV).
- Spectrum rises again mainly because of ^{11}C cosmogenic events.

Results

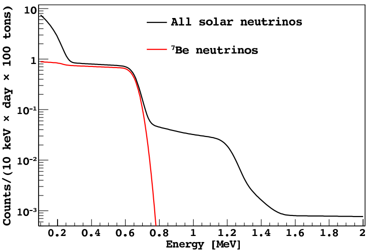

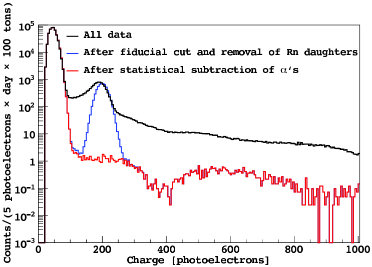

- ^{14}C dominates the spectrum for low energies.
- ^{210}Po peak at 200 pe is intrinsic to scintillator.
- Clear shoulder at 380 pe (approx 750 keV).
- Spectrum rises again mainly because of ^{11}C cosmogenic events.

Results

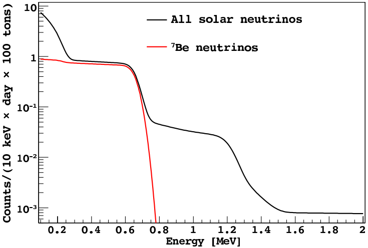

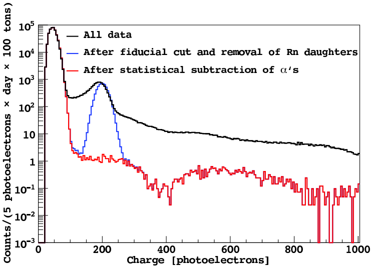

- Interaction rate of ^{7}Be-neutrinos: $47 \pm 7_{stat} \pm 12_{sys}$ counts/(day$\cdot$ 100 ton)
- ^{85}Kr rate: $22 \pm 7 \pm 5$ counts/(day$\cdot$ 100 ton)

The expected rate from the SSM is 49 ± 4 counts/(day$\cdot$ 100 ton) with and 75 ± 4 counts/(day$\cdot$ 100 ton) without oscillations respectively.

Future prospects

- Reduce bg from ^{11}C
- Measurement of *pep* and CNO neutrinos becomes feasible.
- Measurement of geoneutrinos.

Future Perspectives for a Next Generation LS Detector

- Detector for next galactic supernova
- Cosmic diffuse supernova neutrino background spectroscopy
- High statistics neutrino spectroscopy
- Geoneutrino measurement including directionality
- (Search for proton decay)

LENA

Preferred Location:

- Phyäsalmi (Finland)

Other possible locations:

- Pylos (Greece)
- Boulby (UK)
- Canfranc (Spain)
- Fréjus (France)
- Sieroczewice (Poland)
- Henderson (USA)
- Homestake (USA)
- Kimballton (USA)
- Hawaii (USA)

LENA

- Cylindrical shape.
- Length of approx. 100 m.
- Diameter of approx. 30 m.
- Approx 13000 photo-multipliers.
- 50 kt of liquid scintillator.

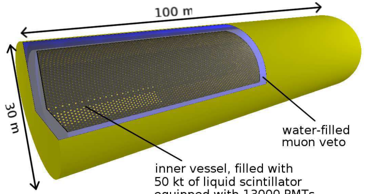

LENA

- Cylindrical shape.
- Length of approx. 100 m.
- Diameter of approx. 30 m.
- Approx 13000 photo-multipliers.
- 50 kt of liquid scintillator.

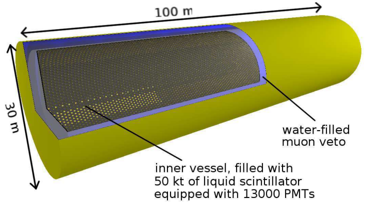

LENA

- Cylindrical shape.
- Length of approx. 100 m.
- Diameter of approx. 30 m.
- Approx 13000 photo-multipliers.
- 50 kt of liquid scintillator.

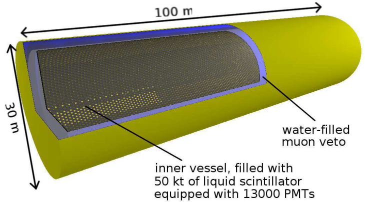

LENA

- Cylindrical shape.
- Length of approx. 100 m.
- Diameter of approx. 30 m.
- Approx 13000 photo-multipliers.
- 50 kt of liquid scintillator.

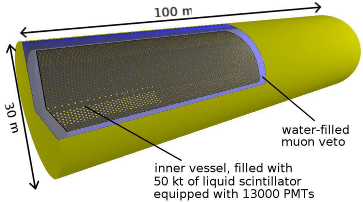

Detector Design

- PXE as scintillator
- Admixture of dodecane increases number of protons (25%) and enhances optical properties
- Attenuation length of 12 m at 450 nm wavelength can be reached.
- Non hazardous, flash-point at 145°C.

Borexino and KamLAND show that LS can be well handled!

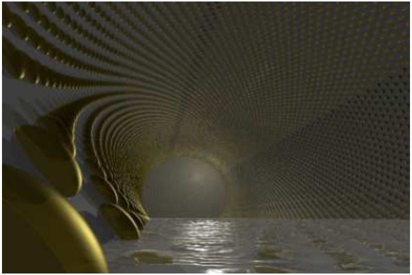

Summary and Outlook

- Liquid Scintillators offer an excellent detection method for low energy neutrinos.
- $\bar{\nu}_e$-oscillations have been confirmed in KamLAND.
- Successful detection of geoneutrinos
- ^{7}Be-ν_e from the Sun have been observed in Borexino
- Plans for a 50 kton LS detector look promising

Summary and Outlook

- Liquid Scintillators offer an excellent detection method for low energy neutrinos.
- $\bar{\nu}_e$-oscillations have been confirmed in KamLAND.
- Successful detection of geoneutrinos
- ^{7}Be-ν_e from the Sun have been observed in Borexino
- Plans for a 50 kton LS detector look promising

Summary and Outlook

- Liquid Scintillators offer an excellent detection method for low energy neutrinos.
- $\bar{\nu}_e$-oscillations have been confirmed in KamLAND.
- Successful detection of geoneutrinos
- ^{7}Be-ν_e from the Sun have been observed in Borexino
- Plans for a 50 kton LS detector look promising

Summary and Outlook

- Liquid Scintillators offer an excellent detection method for low energy neutrinos.
- $\bar{\nu}_e$-oscillations have been confirmed in KamLAND.
- Successful detection of geoneutrinos
- ^{7}Be-ν_e from the Sun have been observed in Borexino
- Plans for a 50 kton LS detector look promising

Summary and Outlook

- Liquid Scintillators offer an excellent detection method for low energy neutrinos.
- $\bar{\nu}_e$-oscillations have been confirmed in KamLAND.
- Successful detection of geoneutrinos
- ^{7}Be-ν_e from the Sun have been observed in Borexino
- Plans for a 50 kton LS detector look promising